

Coulomb impurities in graphene driven by fast ions

Saparboy Rakhmanov,¹ Reinhold Egger,² Doniyor Jumanazarov,^{3,4} and Davron Matrasulov^{5,6}

¹*Chirchik State Pedagogical University, 104 Amur Temur Str., 111700 Chirchik, Uzbekistan*

²*Institut für Theoretische Physik, Heinrich-Heine-Universität, 40225 Düsseldorf, Germany*

³*Department of Physics, Urgench State University, Urgench 220100, Uzbekistan*

⁴*Department of Telecommunication Engineering, Urgench Branch of Tashkent University of Information Technologies, Urgench 220100, Uzbekistan*

⁵*Turin Polytechnic University in Tashkent, 17 Niyazov Str., 100095 Tashkent, Uzbekistan*

⁶*Center for Theoretical Physics, Khazar University, 41 Mehseti Street, Baku, AZ1096, Azerbaijan*

We provide a theoretical model for electronic transitions in a two-dimensional (2D) artificial atom in a graphene monolayer. The artificial atom is due to the presence of a charged adatom (Coulomb impurity) in the layer and interacts with a fast ultrarelativistic ion moving parallel to the layer. We compute the probability and cross sections for the corresponding electronic transitions by means of an exact solution of the time-dependent 2D Dirac equation describing the interaction of the planar atom with the electromagnetic field of the ultrarelativistic projectile.

It is well known that by doping charged impurities into graphene monolayers, one can create artificial planar relativistic atoms described by the Dirac equation [1]. Coulomb impurities in graphene thus provide a powerful testing ground for relativistic quantum mechanics and (2+1) dimensional quantum electrodynamics (QED) [2–9]. In addition, high-energy phenomena such as 2D versions of the electronic transitions induced by relativistic ion-atom collisions can be studied for graphene at the table-top level. For relativistic ion-atom collisions, electronic transitions may appear in the form of excitation, ionization and/or electron-positron (*aka* electron-hole) creation processes. In the conventional 3D case, such high-energy collision phenomena can be only probed in collider facilities such as the LHC (CERN) [10], the Relativistic Heavy Ion Collider (Brookhaven) [11, 12], or the FAIR facility at GSI [13–15].

In this work, we consider an artificial atom due to a Coulomb impurity with charge $Z_T e$ in the graphene layer. The atom interacts with a fast ion of charge $Z_P e$ moving parallel to the graphene layer at perpendicular distance b and speed v , see Fig. 1 for an illustration. We use coordinates where the xz plane represents the graphene layer, the Coulomb impurity is centered at $x = z = 0$, and the ion propagates along the z direction with $x = 0$ and $y = b$. We study the electronic transitions induced in the artificial atom by the sudden perturbation of the time-dependent Coulomb field generated by the ion. Our study has been inspired by a series of works by Baltz and co-authors [16–25], where the probabilities and cross-sections of different electronic transitions induced by the collision of a relativistic atom with a fast charged ion have been computed. Considering the ultrarelativistic limit of the projectile’s velocity, Baltz *et al.* have obtained an exact solution of the time-dependent Dirac equation describing the interaction of a fast ion with the relativistic atom. We here consider the 2D counterpart of their analysis.

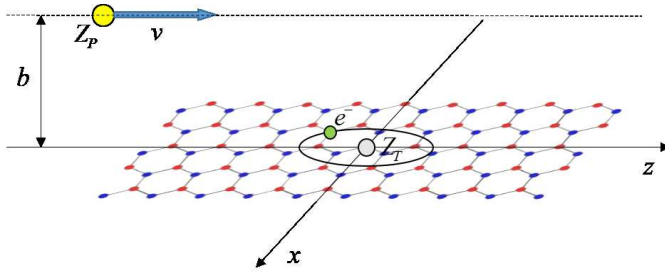


FIG. 1. Schematic sketch of the geometry studied in this paper. A fast charged projectile, represented by an ion with charge $Z_P e$, moves parallel to the graphene layer at perpendicular distance b and speed v . The ion interacts with an artificial 2D atom realized by doping an adatom with charge $Z_T e$ (Coulomb impurity) into the layer. The graphene layer here corresponds to the xz plane, with the artificial atom at the origin. The ion trajectory is assumed to be at $x = 0$, with the velocity pointing along the z direction.

Relativistic 2D atom in graphene driven by a fast ion.— Coulomb impurities in graphene have attracted much attention as condensed matter based realizations of relativistic quantum physics and (2 + 1) dimensional QED. Basic mechanisms for generating vacuum polarization effects (such as quasiparticle pair creation) induced by time-dependent electromagnetic fields have been studied theoretically in Refs. [26–37]. In particular, the critical charge for supercriticality, at which the lowest bound-state energy level dives into the filled Dirac sea, turns out to be much lower than for 3D atoms [27, 28]. In the absence of the ion beam, the artificial 2D atom in graphene has been described in terms of the Dirac equation by Novikov [27], where both the discrete spectrum and the scattering states have been calculated. Following Ref. [27], we first briefly recall the Dirac equation

for the electronic motion in graphene in the presence of a Coulomb impurity. For the vacuum counterpart of this system, see Ref. [28]. Allowing for a homogeneous quasiparticle energy gap M , which could be generated by strain effects due to an underlying substrate, the low-energy Hamiltonian is given by [1, 26, 27]

$$H_0 = v_F(\sigma_x p_x + \sigma_z p_z) + M\sigma_z - \frac{v_F \alpha_{gr} Z_T}{r} \sigma_0. \quad (1)$$

Here $v_F \approx c/300$ denotes the Fermi velocity in ungapped graphene (c is the velocity of light), Z_{TE} is the charge of the Coulomb impurity (target), and $\alpha_{gr} \sim \mathcal{O}(1)$ is the effective fine structure constant of the graphene layer which depends on the dielectric constant of the substrate. The Pauli matrices $\sigma_{x,z}$ (with identity σ_0) act in sublattice space for graphene's honeycomb lattice [1]. We use $\mathbf{r} = (x, z)$, $r = \sqrt{x^2 + z^2}$, and $p_{x,z} = -i\partial_{x,z}$. For clarity, we consider a single K valley of the band structure and a single spin polarization. These assumptions are justified if the electromagnetic field generated by the ion pulse varies smoothly in space on the scale of the lattice constant ($a_0 \sim 2.46 \text{ \AA}$) [1].

In the absence of external fields, the quasiparticle spinor wave function obeys the stationary Dirac equation, $H_0|\psi\rangle = E|\psi\rangle$. Following Refs. [27, 28], we separate angular (ϕ) and radial (r) variables,

$$\psi_{n,j}(\mathbf{r}) = \begin{pmatrix} F_{n,j}(r) \Phi_{j-1/2}(\phi) \\ iG_{n,j}(r) \Phi_{j+1/2}(\phi) \end{pmatrix}, \quad (2)$$

where the integers n and half-integers j are the principal and angular momentum quantum numbers, respectively. With integer m , the angular eigenfunctions are $\Phi_m(\phi) = \frac{1}{\sqrt{2\pi}} e^{im\phi}$. The radial eigenfunctions $F_{n,j}(r)$ and $G_{n,j}(r)$ are specified in closed form in Ref. [27]. We here focus on the discrete spectrum, $|E| < M$. Assuming $0 \leq \alpha_{gr} Z_T < 1/2$ throughout, the respective bound-state eigenenergies are

$$E_{n,j} = \frac{M}{\sqrt{1 + \frac{\alpha_{gr}^2 Z_T^2}{(n+\gamma_j)^2}}}, \quad \gamma_j = \sqrt{j^2 - \alpha_{gr}^2 Z_T^2}, \quad (3)$$

where $n \geq 0$ for $j > 0$, and $n > 0$ for $j < 0$.

We next include the effects of the ion beam on the target described by H_0 . For the conventional 3D counterpart, electronic transitions induced by collisions of fast (ultra-relativistic, $v \approx c$) ions with atoms have attracted much attention during the past three decades in atomic and high energy physics [38–41]. In particular, the 3D counterpart of the model studied below for the 2D graphene case was studied in Refs. [20, 22, 23]. We here adapt these calculations to 2D artificial atoms, see Fig.1, and

discuss the corresponding physical observables. Following the arguments in Ref. [23], the time-dependent potential created by the moving ion (projectile) of charge Z_{PE} on the target electron is then given by

$$V(x, z, t) = -\delta(z - ct) \alpha Z_P (1 - \sigma_z) \ln \left(1 + \frac{x^2}{b^2} \right), \quad (4)$$

where b is the impact parameter and $\alpha \simeq 1/137$ the standard fine structure constant. The dynamics of the complete projectile-plus-target system is thus described by the time-dependent Dirac equation

$$i \frac{\partial \Psi(\mathbf{r}, t)}{\partial t} = [H_0 + V(\mathbf{r}, t)] \Psi(\mathbf{r}, t), \quad (5)$$

with H_0 in Eq. (1). We recall that $\mathbf{r} = (x, z)$ is the electron position corresponding to the target atom.

As for the 3D counterpart [23], the solution of Eq. (5) can be obtained by expanding $\Psi(\mathbf{r}, t)$ in terms of the complete set of eigenfunctions of H_0 ,

$$\Psi(\mathbf{r}, t) = \sum_l a_l(t) \psi_l(\mathbf{r}) e^{-iE_l t}, \quad (6)$$

where $a_l(t)$ are complex-valued and time-dependent expansion coefficients. The index l includes the quantum numbers n and j in Eq. (2). Substituting Eq. (6) into Eq. (5), we find that the coefficient $a_f(t)$ for the final state $|\psi_f\rangle$ is governed by

$$\frac{da_f(t)}{dt} = -i e^{iE_f t} \langle \psi_f | V(\mathbf{r}, t) | \psi_i \rangle, \quad (7)$$

where we assumed that prior to the interaction, the atomic electron was in the state $|\psi_i\rangle$, i.e.,

$$\Psi_i(\mathbf{r}, t \rightarrow -\infty) = e^{-iE_i t} \psi_i(\mathbf{r}). \quad (8)$$

Equation (7) thus comes with the initial condition

$$a_f(t \rightarrow -\infty) = \delta_{f,i}. \quad (9)$$

In order to obtain the exact solution of Eq. (7) with $V(x, z, t)$ in Eq. (4), it suffices to determine $\Psi(\mathbf{r}, t)$ near $z = ct$ [23]. We therefore transform to light-cone coordinates,

$$z^- = \frac{1}{\sqrt{2}}(ct - z), \quad z^+ = \frac{1}{\sqrt{2}}(ct + z). \quad (10)$$

For $t < z/c$ but very close to $t = z/c$, by integrating Eq. (5) over z^- , taking into account the $\delta(z^-)$ function and the Heaviside step function $\theta(z)$ with $\frac{d}{dz} \exp \theta(z) = \delta(z) \exp \theta(z)$, we obtain

$$(1 - \sigma_z) \Psi_i(\mathbf{r}, t) = (1 - \sigma_z) e^{-i\theta(ct-z)} \alpha Z_P \ln(1+x^2/b^2) \psi_i(\mathbf{r}) e^{-iE_i t}. \quad (11)$$

Next we substitute Eq. (11) into Eq. (7) and integrate over time. Taking into account the initial condition (9), we obtain the transition amplitude $a_{f,i} = a_f(t \rightarrow \infty)$ as

$$a_{f,i} = \delta_{f,i} - i \int_{-\infty}^{\infty} dt e^{i(E_f - E_i)t} \langle \psi_f | \delta(z - ct) \alpha Z_P (1 - \sigma_z) \ln \left(1 + \frac{x^2}{b^2} \right) | e^{-i\theta(ct-z)\alpha Z_P \ln(1+x^2/b^2)} \psi_i \rangle. \quad (12)$$

Performing the t -integration, we obtain the final result

$$a_{f,i} = \delta_{f,i} + \langle \psi_f | (1 - \sigma_z) e^{i(E_f - E_i)z/c} (e^{-i\alpha Z_P \ln(1+x^2/b^2)} - 1) | \psi_i \rangle. \quad (13)$$

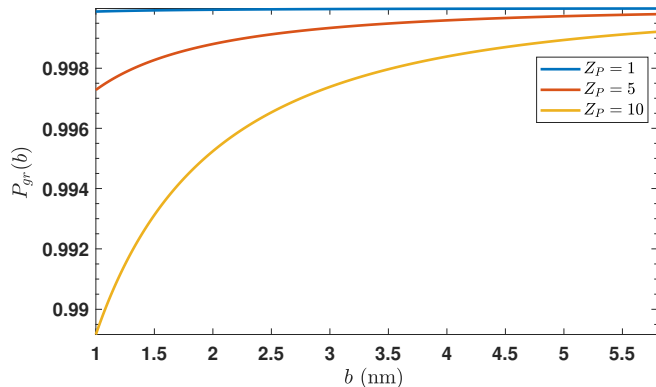


FIG. 2. Survival probability in the ground state of the artificial atom, see Eq. (14), vs impact parameter b at different values of the projectile charge Z_P in Eq. (4) for $\alpha_{gr} Z_T = 0.4$, $M \approx 0.1$ eV and $v_F = c/300$. Note the logarithmic scale for the probabilities.

Equation (13) gives the transition amplitude of the target atom from the initial state $|\psi_i\rangle$ to the final state $|\psi_f\rangle$ induced by its interaction with the fast ion with charge Z_P . This expression has been derived by assuming that the projectile's velocity is close to the speed of light, $v \lesssim c$. We next use this expression for calculating the probabilities and cross-sections for excitation and ionization.

Probabilities and cross sections for electronic transitions.—We now present results for the probabilities and cross sections of target electron transitions based on the exact expression in Eq. (13). Our calculations use the so-called survival or staying probability of the target electron in its initial state. The survival probability is the probability that the electron remains in its initial state during the interaction with the external perturbation. Taking into account $E_f - E_i = 0$, from Eq. (13), the survival probability can be written as

$$P_i(b) = \left| 1 + \langle \psi_i | (1 - \sigma_z) \left(e^{-i\alpha Z_P \ln(1+x^2/b^2)} - 1 \right) | \psi_i \rangle \right|^2. \quad (14)$$

Similarly, for the transition probability from an initial state $|\psi_i\rangle$ to the final state, $|\psi_f\rangle$ (with $f \neq i$), we obtain

$$P_{f,i}(b) = \left| \langle \psi_f | (1 - \sigma_z) e^{i(E_f - E_i)z/c} \left(e^{-i\alpha Z_P \ln(1+x^2/b^2)} - 1 \right) | \psi_i \rangle \right|^2. \quad (15)$$

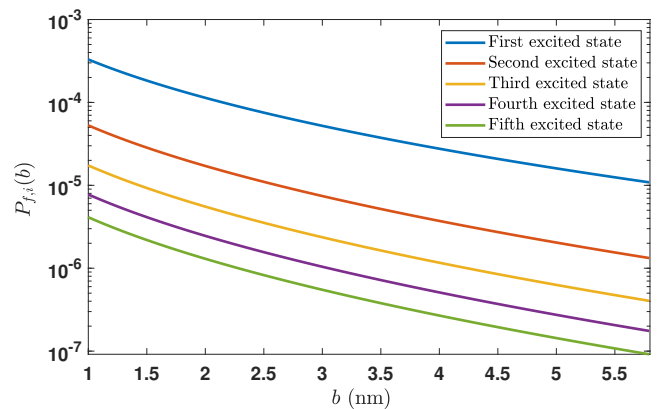


FIG. 3. Excitation probability (15) vs impact parameter b from the ground state of the artificial atom to the first five excited states due to the interaction with an ultrarelativistic ion with $Z_P = 10$ for $Z_T \alpha_{gr} = 0.4$. The other parameters are as specified in the caption to Fig. 2. Note the logarithmic scale for the probabilities.

In Figure 2, the survival probability (14) of the target ground state is plotted as a function of the impact parameter b for different values of the projectile charge Z_P . We observe that the survival probability grows rapidly within a small range of b , saturating at the maximal value $P_i(b) = 1$ at large b . Upon increasing the projectile charge, the staying probability is seen to decrease. Both observations are in agreement with intuitive expectations.

Next, in Figure 3, we show the excitation probabilities (15) from the ground state to the first five excited states of the artificial atom. Unlike the survival probability, a rapid decline of the probability with increasing impact parameter b is observed. This decrease of the excitation probability is approximately exponential in b , at least for not too small b , which can be rationalized by the finite energy differences between the ground state and the respective excited states. In addition, the respective probabilities decrease with increasing order of the excited state.

According to the unitarity principle, the sum of the survival, the excitation (bound states) and the ionization (continuum states) transition probabilities should give unity. This fact implies that the total ionization probability (summed over all continuum states), $P(b)$, can be computed without explicit calculation of the respec-

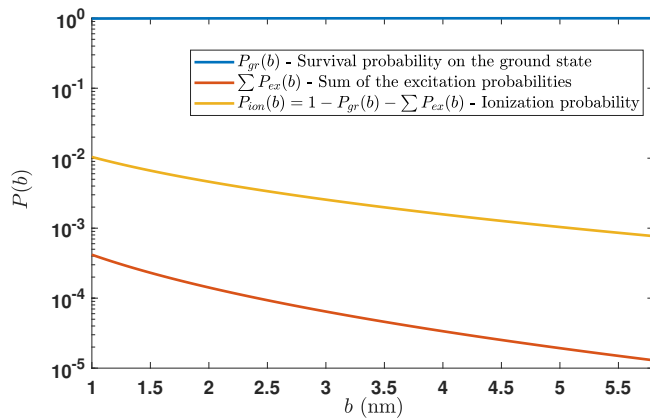


FIG. 4. Survival probability (14), the sum of the excitation probabilities (15) to excited bound states, and the total ionization probability (16) vs impact parameter b for $Z_P = 10$ and $Z_T \alpha_{gr} = 0.4$. Note the logarithmic scale for the probabilities. The other parameters are as in Fig. 2.

Z_P	σ (barn)
1	2.76×10^7
5	6.88×10^8
10	2.74×10^9

TABLE I. Ionization cross section (17) of the artificial atom for several values of the ion charge parameter Z_P . The same parameters as specified in Fig. 2 have been used.

tive transition amplitudes using the scattering state wave functions, see also Ref. [16]. The total ionization probability thus follows as

$$P(b) = 1 - P_i(b) - \sum_{f \neq i} P_{f,i}(b), \quad (16)$$

where the sum over f extends over all bound states of the artificial atom except for the ground state. In Fig. 4, we show the survival probability, the sum of the excitation probabilities, and the total ionization probability as a function of the impact parameter b . For the total excitation and ionization probabilities, we find a decay of the probability as b increases. Importantly, the total ionization probability exceeds the total excitation probability by several orders of magnitude, especially for large b .

From the total ionization probability $P(b)$, the total ionization cross section follows by integrating over the impact parameter [16],

$$\sigma = 2\pi \int_0^\infty db b P(b). \quad (17)$$

In Table I, we provide the resulting values of the ionization cross section for different values of the projectile charge parameter Z_P . Comparing the values of the cross section to those for the 3D counterpart [16], the cross section is found to be two orders of magnitude larger.

As expected, upon increasing Z_P , the cross section also increases substantially.

Conclusions.—In this work, we have considered a low-energy theory for a Coulomb impurity in a graphene monolayer interacting with a fast (ultrarelativistic) ion moving parallel to the graphene sheet at distance b . The exact solution of the time-dependent 2D Dirac equation describing the interaction of the target artificial atom (which is created by the Coulomb impurity) with the ultrarelativistic charged projectile is obtained. Using this solution, the electronic transition probabilities to excited bound states, the survival probability in the ground state, and the total ionization probability have been analyzed as function of the impact parameter b . In addition, we have computed the cross section which is found to be two orders larger than its 3D counterpart. Probing collision-induced electronic transitions in the planar atoms formed by Coulomb impurities in graphene formed offers interesting perspectives for future experiments.

Let us also mention that the above approach can be applied for the calculation of arbitrary electronic transitions, including particle-hole pair creation processes and the angular distribution of differential cross sections. An interesting extension of our study is to investigate the supercritical case $\alpha_{gr} Z_T > 1/2$, see, e.g., Refs. [3, 5, 8, 42, 43]. In this case as the target state wave functions one can use those obtained in the Refs. [5, 8, 42]. The final state wave function (for excitation) one can use either discrete state eigenvalues of the Dirac operator given by (1), or plane wave states considered in [27]. All these can be done within the above approach. Experimentally, the above model could be realized by passing a fast charged ion (e.g. proton) beam over the graphene layer, as schematically presented in Fig. 5.

Acknowledgements.—We acknowledge funding by the Grant REP-05032022/235 (“Ultrafast phenomena and vacuum effects in relativistic artificial atoms created in graphene”), funded under the MUNIS Project, supported by the World Bank and the Government of the Republic of Uzbekistan. The work of DM is supported by the grant of the Ministry for Higher Education, Research and

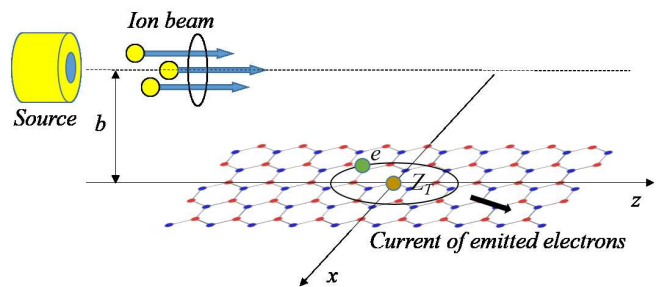


FIG. 5. Sketch for a possible experimental realization of the setup studied in this work.

-
- [1] A. H. Castro Neto, F. Guinea, N. M. R. Peres, K. S. Novoselov, and A. K. Geim, The electronic properties of graphene, *Rev. Mod. Phys.* **81**, 109 (2009).
- [2] A. Luican-Mayer, M. Kharitonov, G. Li, C.-P. Lu, I. Skachko, A.-M. B. Gonçalves, K. Watanabe, T. Taniguchi, and E. Y. Andrei, Screening Charged Impurities and Lifting the Orbital Degeneracy in Graphene by Populating Landau Levels, *Phys. Rev. Lett.* **112**, 036804 (2014).
- [3] Y. Wang, D. Wong, A. V. Shytov, V. W. Brar, S. Choi, Q. Wu, H.-Z. Tsai, W. Regan, A. Zettl, R. K. Kawakami, S. G. Louie, L. S. Levitov, and M. F. Crommie, Observing Atomic Collapse Resonances in Artificial Nuclei on Graphene, *Science* **340**, 734 (2013).
- [4] Y. Wang, V. W. Brar, A. V. Shytov, Q. Wu, W. Regan, H.-Z. Tsai, A. Zettl, L. S. Levitov, and M. F. Crommie, Mapping Dirac quasiparticles near a single Coulomb impurity on graphene, *Nature Physics* **8**, 653 (2012).
- [5] V. M. Pereira, J. Nilsson, and A. H. Castro Neto, Coulomb Impurity Problem in Graphene, *Phys. Rev. Lett.* **99**, 166802 (2007).
- [6] O. V. Gamayun, E. V. Gorbar, and V. P. Gusynin, Supercritical Coulomb center and excitonic instability in graphene, *Phys. Rev. B* **80**, 165429 (2009).
- [7] A. De Martino, D. Klöpfer, D. Matrasulov, and R. Egger, Electric-Dipole-Induced Universality for Dirac Fermions in Graphene, *Phys. Rev. Lett.* **112**, 186603 (2014).
- [8] D. Klöpfer, A. De Martino, and R. Egger, Bound States and Supercriticality in Graphene-Based Topological Insulators, *Crystals* **3**, 14 (2013).
- [9] S. Rakhmanov, R. Egger, and D. Matrasulov, Coulomb impurities in graphene driven by ultrashort electromagnetic pulses: excitation, ionization, and pair creation, *Phys. Scr.* **99**, 075953 (2024).
- [10] T. Renk and K. J. Eskola, Hard dihadron correlations in heavy-ion collisions at energies available at the BNL Relativistic Heavy Ion Collider and CERN Large Hadron Collider, *Phys. Rev. C* **84**, 054913 (2011).
- [11] M. I. Abdulhamid, and et al., Exclusive J/ψ , $\psi(2s)$ and e^+e^- pair production in Au+Au ultraperipheral collisions at the BNL Relativistic Heavy Ion Collider, *Phys. Rev. C* **110**, 014911 (2024).
- [12] J. Adam and et al., Beam energy dependence of net- Λ fluctuations measured by the STAR experiment at the BNL Relativistic Heavy Ion Collider, *Phys. Rev. C* **102**, 024903 (2020).
- [13] T. Stöhlker, Y. A. Litvinov, and for the SPARC Collaboration, Atomic physics experiments at the high energy storage ring, *Physica Scripta* **2015**, 014025 (2015).
- [14] P. M. Hillenbrand, S. Haggmann, T. Stöhlker, Y. Litvinov, C. Kozhuharov, U. Spillmann, V. Shabaev, K. Stiebing, M. Lestinsky, A. Surzhykov, A. Voitkiv, B. Franzke, D. Fischer, C. Brandau, S. Schippers, A. Mueller, D. Schneider, D. Jakubassa, A. Artiomov, E. DeFilippo, X. Ma, R. Dorner, and H. Rothard, Future experiments using forward electron spectroscopy to study the quantum dynamics of high-Z ions at the ESR/CRYRING storage rings, *Physica Scripta* **2013**, 014087 (2013).
- [15] S. Haggmann, T. Stöhlker, Y. Litvinov, C. Kozhuharov, P.-M. Hillenbrand, U. Spillmann, V. Shabaev, K. Stiebing, M. Lestinsky, A. Surzhykov, A. Voitkiv, B. Franzke, D. Fischer, D. Schneider, D. Jakubassa, A. Artiomov, E. DeFilippo, X. Ma, R. Dörner, and H. Rothard, Few-body quantum dynamics of high-Z ions studied at the future relativistic high-energy storage ring, *Physica Scripta* **2013**, 014086 (2013).
- [16] A. J. Baltz, Exact Dirac-equation calculation of ionization induced by ultrarelativistic heavy ions, *Phys. Rev. A* **61**, 042701 (2000).
- [17] A. J. Baltz, Some exact analytical results and a semiempirical formula for single electron ionization induced by ultrarelativistic heavy ions, *Phys. Rev. A* **64**, 022718 (2001).
- [18] A. J. Baltz, Coulomb corrections in the calculation of ultrarelativistic heavy ion production of continuum electron-positron pairs, *Phys. Rev. C* **68**, 034906 (2003).
- [19] A. J. Baltz, Calculation of heavy ion pair production to all orders in $Z\alpha$, *Phys. Rev. C* **71**, 024901 (2005).
- [20] A. J. Baltz, M. J. Rhoades-Brown, and J. Weneser, Energy dependence of bound-electron-positron pair production at very-high-energy ion-ion transits, *Phys. Rev. A* **44**, 5569 (1991).
- [21] A. J. Baltz, M. J. Rhoades-Brown, and J. Weneser, Bound-electron-positron pair production in relativistic heavy-ion collisions, *Phys. Rev. A* **47**, 3444 (1993).
- [22] A. J. Baltz, Coulomb potential from a particle in uniform ultrarelativistic motion, *Phys. Rev. A* **52**, 4970 (1995).
- [23] A. J. Baltz, Exact Dirac Equation Calculation of Ionization and Pair Production Induced by Ultrarelativistic Heavy Ions, *Phys. Rev. Lett.* **78**, 1231 (1997).
- [24] A. J. Baltz and L. McLerran, Two center light cone calculation of pair production induced by ultrarelativistic heavy ions, *Phys. Rev. C* **58**, 1679 (1998).
- [25] A. J. Baltz, M. J. Rhoades-Brown, and J. Weneser, Calculation of the cross section for e^+e^- (K orbit) pairs by very-high-energy fully stripped heavy ions at perturbational impact parameters, *Phys. Rev. A* **48**, 2002 (1993).
- [26] V. N. Kotov, B. Uchoa, V. M. Pereira, F. Guinea, and A. H. Castro Neto, Electron-Electron Interactions in Graphene: Current Status and Perspectives, *Rev. Mod. Phys.* **84**, 1067 (2012).
- [27] D. S. Novikov, Elastic scattering theory and transport in graphene, *Phys. Rev. B* **76**, 245435 (2007).
- [28] V. R. Khalilov and C.-L. Ho, *Mod. Phys. Lett. A* **13**, 615 (1998).
- [29] D. Allor, T. D. Cohen, and D. A. McGady, Schwinger mechanism and graphene, *Phys. Rev. D* **78**, 096009 (2008).
- [30] M. Lewkowicz and B. Rosenstein, Dynamics of Particle-Hole Pair Creation in Graphene, *Phys. Rev. Lett.* **102**, 106802 (2009).
- [31] M. Lewkowicz, H. C. Kao, and B. Rosenstein, Signature of the Schwinger pair creation rate via radiation generated in graphene by a strong electric current, *Phys. Rev. B* **84**, 035414 (2011).
- [32] G. L. Klimchitskaya and V. M. Mostepanenko, Creation

- of quasiparticles in graphene by a time-dependent electric field, *Phys. Rev. D* **87**, 125011 (2013).
- [33] F. Fillion-Gourdeau and S. MacLean, Time-dependent pair creation and the Schwinger mechanism in graphene, *Phys. Rev. B* **92**, 035401 (2015).
- [34] I. Akal, R. Egger, C. Müller, and S. Villalba-Chávez, Simulating dynamically assisted production of Dirac pairs in gapped graphene monolayers, *Phys. Rev. D* **99**, 016025 (2019).
- [35] I. Akal, R. Egger, C. Müller, and S. Villalba-Chávez, Low-dimensional approach to pair production in an oscillating electric field: Application to bandgap graphene layers, *Phys. Rev. D* **93**, 116006 (2016).
- [36] A. Golub, R. Egger, C. Müller, and S. Villalba-Chávez, Dimensionality-driven photoproduction of massive dirac pairs near threshold in gapped graphene monolayers, *Phys. Rev. Lett.* **124**, 110403 (2020).
- [37] S. Villalba-Chávez, O. Mathiak, R. Egger, and C. Müller, Light-amplified Landau-Zener conductivity in gapped graphene monolayers: A simulacrum of photocatalyzed vacuum instability, *Phys. Rev. D* **108**, 116007 (2023).
- [38] J. Eichler and T. Stöhlker, Radiative electron capture in relativistic ion-atom collisions and the photoelectric effect in hydrogen-like high- Z systems, *Phys. Rep.* **439**, 1 (2001).
- [39] J. Eichler, Theory of relativistic ion-atom collisions, *Phys. Rep.* **193**, 165 (1990).
- [40] D. Dewangan and J. Eichler, Charge exchange in energetic ion-atom collisions, *Phys. Rep.* **247**, 59 (1994).
- [41] J. Eichler, *Relativistic atomic collisions* (San Diego: Academic Press, 1995).
- [42] M. Asorey and A. Santagata, The critical transition of coulomb impurities in gapped graphene, *J. High Energ. Phys.* **2020**, 144 (2020).
- [43] V. M. Kuleshov, V. D. Mur, and N. B. Narozhny, Coulomb problem for graphene with supercritical impurity, *J. Phys.: Conf. Ser.* **788**, 012044 (2017).